

Optical Transitions in Ruby across the Corundum to Rh₂O₃ (II) Phase Transformation

Wenhui Duan,¹ G. Paiva,^{1,2} Renata M. Wentzcovitch,^{1,2} and A. Fazzio²

¹*Department of Chemical Engineering and Materials Science, and Minnesota Supercomputer Institute, University of Minnesota, Minneapolis, Minnesota 55455*

²*Instituto de Física, Universidade de São Paulo, CP 66318, 5389-970, São Paulo, SP, Brazil*

(Received 27 April 1998)

First principles calculations of a substitutional chromium impurity in Al₂O₃ and analysis of its multiplet structure reveal that the major effect of the corundum to Rh₂O₃ (II) phase transformation in ruby's optical transitions should be a redshift of the broad *U* and *Y* absorption lines across the transformation. A similar phenomenon is experimentally detected above 30 GPa, which is too low a pressure to attribute this phenomenon to a phase transition in the host. However, an anomalous relaxation around the impurity in corundum could explain the observed frequency shifts. The underlying cause of such abnormal relaxation could be a similar transformation in Cr₂O₃ taking place below 30 GPa. The centroids of the *R*, *R'*, and *B* lines are quite insensitive to the transformation. [S0031-9007(98)07269-X]

PACS numbers: 78.55.Hx, 61.50.Ks, 61.72.Ji, 62.50.+p

Ruby, or Cr-doped alumina, is a material of central importance to high pressure science. The pressure dependence of its fluorescence lines serves routinely as a pressure gauge in diamond anvil cell (DAC) experiments. The so called “*ruby pressure scale*” [1] is particularly popular because of the simplicity and accuracy of optical measurements through the DAC's transparent windows, and much effort has gone into improving its accuracy [2,3]. Although it has been calibrated up to 180 GPa [2], pressures as high as 4–5 Mbar have been inferred from observed line shifts [4]. In the past, the scale calibration beyond 180 GPa has been impeded by difficulties in exciting and measuring the fluorescence. However, direct excitation of the fluorescence lines has recently been demonstrated to 250 GPa [5], opening up the possibility of a scale calibration in the multimegabar range.

Within the last decade, several theoretical predictions of a phase transformation from corundum to the Rh₂O₃ (II) phase have been made [6,7], but corundum seemed to remain stable up to 175 GPa at room temperature [8]. Recently, this phase transformation has been observed at approximately 100 GPa and 1000 K [9]. Besides, a second high pressure transformation, as yet unobserved, to the *Pbnm*-perovskite phase is predicted to take place at 223 ± 10 GPa [7]. This raises new concerns about the meaning of the fluorescence spectrum of ruby in the Mbar regime, especially if ruby is inadvertently heated in the DAC. In this paper we investigate the effects of pressure and of the newly found phase transformation on ruby's optical transitions. We combine a first principles calculation of the chromium impurity, a *color center*, with an analytical multiplet approach capable of separating mean field from many electron effects [10].

The present calculation builds on previous first principles studies of the alumina host lattices [7,11]. The electronic and structural properties of the color center are now obtained by performing fully relaxed supercell

calculations containing one chromium impurity per 80 atoms. Table I compares the atomic arrangement around chromium with those around aluminum in Al₂O₃ and chromium in Cr₂O₃ at zero pressure. The atomic environment of chromium in ruby is found to be intermediate between chromium's in Cr₂O₃ and aluminum's in the host lattice, in agreement with experimental measurements [13–15]. Figure 1 displays two important trends which are valid up to the highest pressures investigated: (1) Lattice relaxation around the impurity decreases rapidly throughout the coordination shells. The interatomic distances between chromium and oxygen in the third coordination shell are essentially the same as those in the host at all pressures [16]. (2) $\overline{\text{Cr-O}}$ and $\overline{\text{Al-O}}$ bond compressibilities differ substantially. This implies that the procedure usually adopted in phenomenological crystal field studies of scaling $\overline{\text{Cr-O}}$ bond lengths by $[V(P)/V(0)]^{1/3}$, where $V(P)$ is the pressure dependent volume of Al₂O₃, is unrealistic, as has been previously noticed [17]. Also, CrO₆ octahedra distort more under pressure as compared to AlO₆ [16].

Figure 2 shows the pressure dependence of the eigenvalue spectra in both phases. The deep states in both gaps derive from Cr-3*d* states and reflect crystal fields with predominantly *O_h* symmetry ($\Delta \gg \delta$). In corundum the local *C₃* symmetry further splits *t_{2g}* states into an *e* doublet and an *a₁* singlet while, in Rh₂O₃ (II), *t_{2g}* and *e_g* derived states are all split (*C₁* point symmetry). These eigenvalues and the corresponding eigenvectors were used to calculate the central quantities that enter into the analysis of the multiplet structure according to the method of Fazzio, Caldas, and Zunger [10]. This method differs from the classical phenomenological approach of Sugano, Tanabe, and Kamimura [18] by formally separating *all* one electron mean field effects from many-electron effects and explicitly incorporating results from first principles calculations. In this approach, the Hamiltonian matrix element between

TABLE I. Zero pressure interatomic distances in Al_2O_3 , ruby, and Cr_2O_3 in the corundum phase. The Al (Cr) site has C_3 symmetry, therefore the nearest O neighbors and Al next nearest neighbors are divided into two sets, O_- and O_+ and $\text{Al}(\text{Cr})_1$ and $\text{Al}(\text{Cr})_2$, respectively. θ_{\pm} is the angle between an $\text{Al}(\text{Cr})-O_{\pm}$ bond and the threefold axis.

	Al_2O_3		This calc	Ruby Other work [13–15]	Cr_2O_3	
	This calc	Expt [30]			This calc	Expt [31]
$\text{Al}-O_-$ (Å)	1.839	1.857	—	—	—	—
$\text{Al}-O_+$ (Å)	1.951	1.969	—	—	—	—
$\text{Al}-\text{Al}_1$ (Å)	2.621	2.654	—	—	—	—
$\text{Al}-\text{Al}_2$ (Å)	2.766	2.794	—	—	—	—
$\text{Cr}-O_-$ (Å)	—	—	1.918	1.91 [13], 1.95 [14], 1.88 [15]	1.980	1.962
$\text{Cr}-O_+$ (Å)	—	—	2.018	2.0 [13], 2.04 [14], 1.93 [15]	2.048	2.012
$\text{Cr}-\text{Al}_1$ (Å)	—	—	2.627	2.70 [13]	—	—
$\text{Cr}-\text{Al}_2$ (Å)	—	—	2.766	2.82 [13]	—	—
$\text{Cr}-\text{Cr}_1$ (Å)	—	—	—	—	2.745	2.649
$\text{Cr}-\text{Cr}_2$ (Å)	—	—	—	—	2.946	2.886
θ_- (deg)	63.13	63.11	64.07	—	62.93	62.43
θ_+ (deg)	47.79	46.73	47.89	—	47.94	48.89

different configurations i and j (symmetrized combinations of Slater determinants) giving rise to a term Γ representing spin plus space symmetries are expressed as

$$D_{ij}^{\Gamma}(m, n; m', n') = \Delta E_{ij}^{\Gamma}(m, n; m', n') + \Delta_{\text{eff}}(m, n)\delta_{ij}.$$

$\Delta_{\text{eff}}(m, n)$ is the excitation energy of configuration

$t_{2g}^m e_g^n$ obtained from density functional calculations, i.e., $E_{\text{tot}}(m, n) - E_{\text{tot}}(m_0, n_0)$, where (m_0, n_0) is the ground state configuration. $\Delta E_{ij}^{\Gamma}(m, n; m', n')$'s are quantities that cannot be directly obtained from density functional calculations. In the octahedral field approximation, these matrix elements depend on ten Coulomb (Slater-Condon) integrals between t_{2g} and e_g orbitals. The matrix elements are expressed in terms of the atomic Racah parameters B and C [19] and orbital deformation parameters λ_e and λ_t [10,20,21].

Figure 3 shows the pressure dependence of excitation energies of various terms in both phases and compares

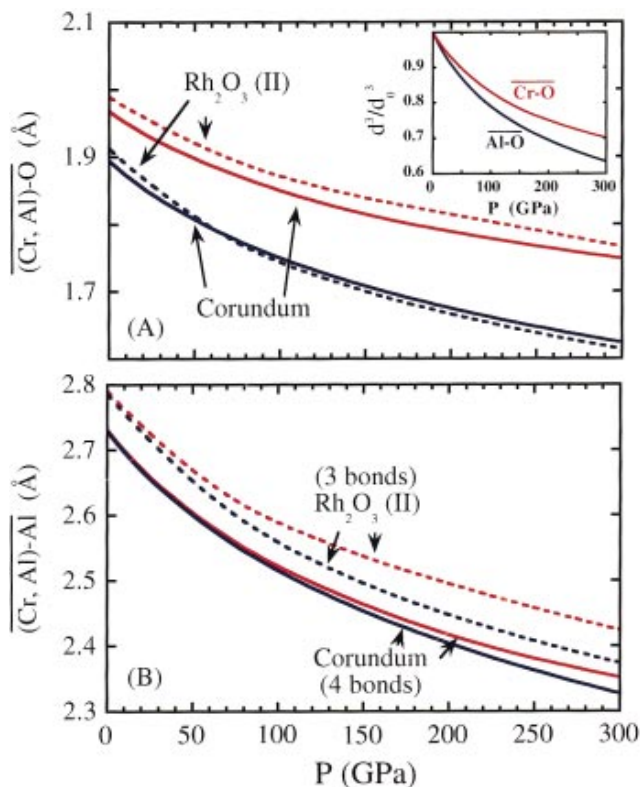


FIG. 1(color). Pressure dependence of the average radii of the (A) first and (B) second coordination shells around chromium in ruby (red) and aluminum in Al_2O_3 (blue) in the corundum (solid) and Rh_2O_3 (II) (dashed) phases. The inset in (A) shows the pressure dependence of the third power of the average nearest neighbor distances $\overline{\text{Cr}-\text{O}}$ (red) and $\overline{\text{Al}-\text{O}}$ (blue) normalized to the zero pressure values.

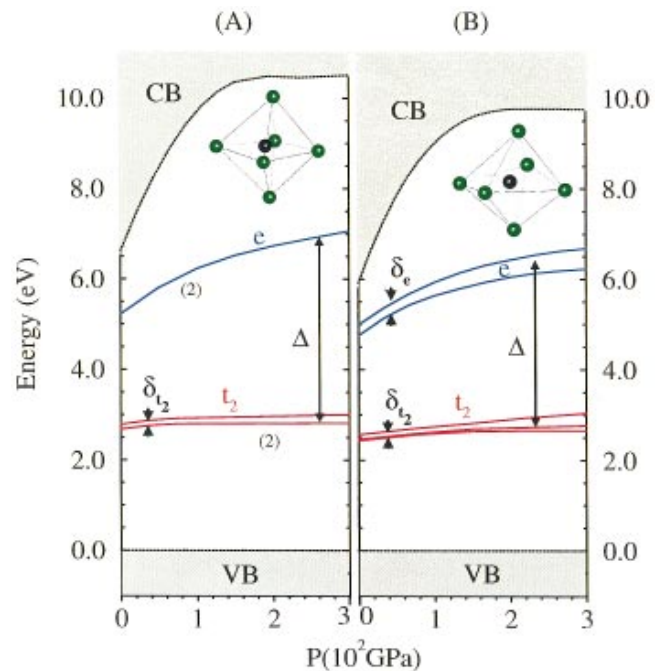


FIG. 2(color). Eigenvalue spectra of Cr-doped Al_2O_3 in (A) corundum and (B) Rh_2O_3 (II) phases. Δ (δ) is the octahedral (trigonal) field splitting.

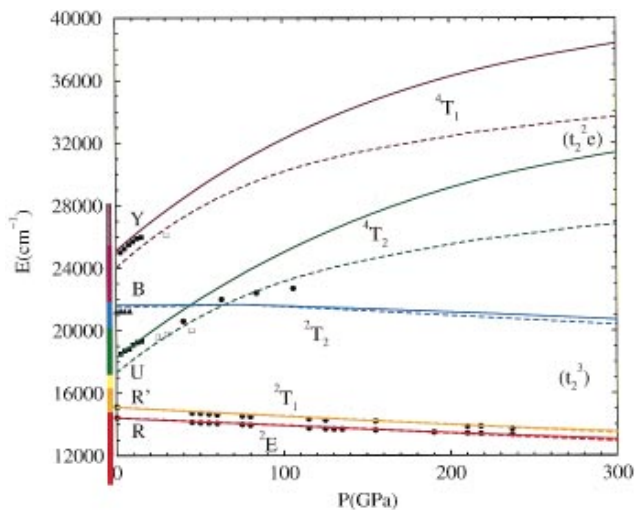


FIG. 3(color). Pressure dependence of the calculated optical transitions in corundum (solid lines) and in Rh_2O_3 (II) (dashed lines) phases. Ground state has 6A_2 symmetry. Experimental data are extracted from Eggert *et al.* [3] (\bullet), Stephens *et al.* [32] (\blacksquare), Forman *et al.* [22] (\blacktriangle), and Goto *et al.* [23] (\square).

them to the centroids of the experimental optical transitions. Several trends can be observed:

(1) The frequency of the luminescent ${}^2E \rightarrow {}^4A_2$ and ${}^2T_1 \rightarrow {}^4A_2$ transitions, and the nonradiative ${}^2T_2 \rightarrow {}^4A_2$ transition, are very similar in both phases throughout the entire pressure range investigated {full (dashed) lines correspond to corundum [Rh_2O_3 (II)] phase}. These transitions, known as the R , R' , and B lines, respectively, are spin forbidden and involve changes between states with predominantly t_{2g}^3 configurations. Our analysis of the matrix elements supports the usual interpretation [18] that the observed pressure induced redshifts of these lines is caused mainly by the increasing degree of delocalization of these states with pressure ($d\lambda_e/dP$ and $d\lambda_l/dP < 0$). In the B line there is a small but noticeable blueshift at low pressures [22]. This is caused by a mixing of t_{2g}^3 and t_{2g}^2e configurations in the 2T_2 term at these pressures. As pressure increases the contribution of the t_{2g}^2e configuration decreases due to the rapid increase in crystal field splitting (Δ), and the effect of delocalization on the excitation energy becomes the predominant one producing a redshift.

(2) The ${}^4A_2 \rightarrow {}^4T_1$ and ${}^4A_2 \rightarrow {}^4T_2$ transitions are spin allowed and give rise to the intense and broad U and Y absorption lines. The excited states are composed predominantly of t_{2g}^2e configurations. The accentuated pressure induced blueshifts of these lines is caused primarily by the direct dependence of the excitation energies on the crystal field splittings, Δ . Figure 2 shows the behavior of the crystal field splittings (Δ) with pressure. In Rh_2O_3 (II) phase Δ is considerably smaller than in corundum at all pressures. Consequently, the U and Y lines should suffer a noticeable redshift across the corundum to Rh_2O_3 (II) transformation. A similar but somewhat less sharp effect

has been noticed experimentally [3,23] and is displayed in Fig. 3. Between 30 and 100 GPa the observed pressure induced blueshift is considerably smaller than that expected based on extrapolations of the low pressure data using a scaled crystal field model [3]. The origin of this effect has been addressed phenomenologically and attributed to spin orbit interaction which couples 4T_2 and 2T_2 states [3], or to a larger pressure induced delocalization of e_g states as compared to t_{2g} [24].

Our results suggest an alternative origin for the observed pressure induced blueshift of the U line, meaning a detectable structural relaxation around chromium that above 30 GPa resembles closely the one expected in the Rh_2O_3 (II) phase, as opposed to that expected in the corundum form. Assuming that Al_2O_3 does not transform to the Rh_2O_3 (II) phase until 80–100 GPa and, even so, requires the aid of high temperatures [9], such anomalous relaxation could originate in an as yet unconfirmed transformation between similar phases in Cr_2O_3 . This could produce an underlying tendency of the chromium neighborhood in corundum to mimic its neighborhood in the Rh_2O_3 (II) phase, especially in the presence of light absorption by chromium and nonradiative decay. The existence of a phase transformation in Cr_2O_3 in this pressure range is considered inconclusive [25], nevertheless resistance and volume anomalies have been reported [26,27] but not confirmed by one x-ray diffraction experiment [28]. These phases are expected to have similar x-ray diffraction patterns [7] and the transformation could have gone unnoticed. Also, our preliminary first principles calculations suggest that this transformation could be taking place below 30 GPa [29]. Other tests of this hypothesis include (1) a simultaneous frequency displacement in the Y line. A discontinuity in frequency shifts seems to exist when comparison is made between all of the experimental data available [3,23], which is quite limited (see Fig. 3). (2) Small but noticeable discontinuities or broadening in the R , R' , and B lines could point towards a symmetry lowering around the chromium site. It appears that these effects cannot be ruled out even in the latest experimental data [3]. (3) Obviously, experimental confirmation of a corundum to Rh_2O_3 (II) phase transformation in Cr_2O_3 would give further support to this hypothesis, but (4) ultimately, the confirmation should come from near edge absorption experiments in ruby.

This research was supported by the Minnesota Supercomputer Institute, the National Science Foundation [award EAR-9628042 (R.M.W.)], and the Brazilian agencies FAPESP and CNPQ. R.M.W. thanks Isaac F. Silveira for a helpful discussion.

- [1] R. A. Forman, G. J. Piermarini, J. D. Barnett, and S. Block, *Science* **176**, 284 (1972).
- [2] H.-K. Mao, J.-A. Xu, and P. M. Bell, *J. Geophys. Res.* **91**, 4637 (1986); P. M. Bell, H.-K. Mao, and K. A. Goettel, *Science* **226**, 542 (1984).

- [3] J. H. Eggert, K. A. Goettel, and I. F. Silvera, *Phys. Rev. B* **40**, 5724 (1989); *ibid.* **40**, 5733 (1989); J. H. Eggert, F. Moshary, W. J. Evans, K. A. Goettel, and I. Silvera, *ibid.* **44**, 7202 (1991).
- [4] J.-A. Xu, H.-K. Mao, and P. M. Bell, *Science* **232**, 1404 (1986); W. C. Moss, J. O. Hallquist, R. Reichlin, K. A. Goettel, and S. Martin, *Appl. Phys. Lett.* **48**, 1258 (1986); Y. K. Vohra, C. A. Vanderborgh, S. Desgreniers, and A. L. Ruoff, *Phys. Rev. B* **42**, 9189 (1990); A. L. Ruoff, H. Xia, and Z. Xia, *Rev. Sci. Instrum.* **63**, 4342 (1992).
- [5] N. Chen and I. F. Silvera, *Rev. Sci. Instrum.* **67**, 4275 (1996).
- [6] H. Cynn, D. G. Isaak, R. E. Cohen, M. F. Nicol, and O. L. Anderson, *Am. Mineral.* **75**, 439 (1990); M. S. T. Bukowinski, A. Chizmeshya, G. H. Wolf, and H. Zhanh, *Mol. Eng.* **6**, 81 (1996); F. C. Marton and R. E. Cohen, *Am. Mineral.* **79**, 789 (1994).
- [7] K. T. Thomson, R. M. Wentzcovitch, and M. S. T. Bukowinski, *Science* **274**, 1880 (1996); W. Duan, R. M. Wentzcovitch, M. Renata, and K. T. Thomson, *Phys. Rev. B* **57**, 10363 (1998). According to this calculation the phase transformation should take place at 78 ± 4 GPa.
- [8] A. P. Jephcoat, R. J. Hemley, H. K. Mao, and K. A. Goettel, *Physica (Amsterdam)* **150B**, 116 (1988).
- [9] N. Funamori and R. Jeanloz, *Science* **278**, 1109 (1997).
- [10] A. Fazzio, M. J. Caldas, and A. Zunger, *Phys. Rev. B* **29**, 5999 (1984); A. Zunger, *Solid State Phys.* **39**, 275 (1986).
- [11] Our density functional calculations used the local density approximation and the same pseudopotentials for oxygen and aluminum as reported earlier [7]. For chromium we generated a pseudopotential with core cutoff radii of $r_s = r_p = 2.5$, $r_d = 1.9$ a.u. (s locality). A plane wave cutoff energy (E_{pw}) of 70 Ry for wave functions (280 Ry for charge density and potential) and one k -point Γ were used. In order to achieve self-consistency in the electronic structure and dynamically stable atomic arrangements around the chromium site it was necessary to occupy the three lowest d -impurity levels in the gap (see Fig. 2) with one electron each. This configuration is a remnant of the naturally observed Cr^{+3} impurity state (spin $+3/2$) and automatically produces the observed point symmetry (C_3). The atomic arrangement around chromium was fully optimized at all pressures [12]. A similar occupation scheme was adopted for calculations in Cr_2O_3 .
- [12] R. M. Wentzcovitch, in *Quantum Theory of Real Materials*, edited by J. R. Chelikowsky and S. G. Louie (Kluwer, Dordrecht, 1996), p. 113.
- [13] P. Kizler, J. He, D. R. Clarke, and P. R. Kenway, *J. Am. Ceram. Soc.* **79**, 3 (1996).
- [14] S. Emura, H. Maeda, Y. Kuroda, and T. Murata, *Jpn. Appl. Phys.* **32**, Suppl. 32-2, 734 (1993).
- [15] S. C. Moss and R. E. Newnham, *Z. Crystall.* **120**, 359 (1964).
- [16] G. Paiva, W. Duan, R. M. Wentzcovitch, and A. Fazzio (to be published). Correct relaxations could have been obtained with smaller supercell calculations {30 (40) atoms in corundum [Rh_2O_3 (II)] phase}; however, the order and degeneracies of the impurity levels, as shown in Fig. 2, required supercells of 80 atoms, presumably due to long ranged impurity interactions.
- [17] S. J. Duclos, Y. K. Vohra, and A. L. Ruoff, *Phys. Rev. B* **41**, 5372 (1990).
- [18] S. Sugano, Y. Tanabe, and H. Kamimura, *Multiplets of Transition Metal Ions in Crystals* (Academic Press, New York, 1970).
- [19] J. S. Griffith, *Theory of Transition Metal Ions* (Cambridge University Press, Cambridge, England, 1961), p. 437.
- [20] R. M. Wentzcovitch, S. L. Richardson, and M. L. Cohen, *Phys. Lett.* **114A**, 203 (1986).
- [21] λ_e and λ_t represent the average ratios between the Coulomb repulsions in the solid and in the free ion for e_g and t_{2g} electrons respectively. The central quantities required to obtain the pressure dependence of the multiplet term energies, i.e., $d\lambda_e/dP$, $d\lambda_t/dP$, and $d\Delta_{\text{eff}}/dP$ for each phase were obtained by first principles. λ 's are approximated and calculated in the solid inside a sphere of radius R_{MT} . The free ion integrals are expressed in terms of the atomic Racah parameters, B and C [19]. The choice of R_{MT} is somewhat arbitrary, and $d\lambda/dP$ is quite insensitive to this choice. Therefore we chose R_{MT} to reproduce an optimum pressure induced redshift for the R' line's centroid. The calculation of λ is described in detail in Refs. [10,20]. Δ_{eff} was calculated using Slater's transition state approximation, i.e., $\Delta_{\text{eff}} = E_{\text{tot}}(t_2^{m-1}e^{n+1}) - E_{\text{tot}}(t_2^m e^n) = \epsilon_e(t^{m-1/2}e^{n+1/2}) - \epsilon_{t_2}(t^{m-1/2}e^{n+1/2})$, where ϵ is one electron eigenvalue. Δ_{eff} and λ were adjusted at zero pressure *only* to reproduce the optical transitions at this pressure in the corundum phase. These adjustments were added to the corresponding zero pressure quantities in the Rh_2O_3 (II) phase. This procedure is justified by the success in obtaining the correct frequencies in the corundum phase at high pressures, i.e., within a wide range of chromium's nearest neighbor distances, including those typical of the Rh_2O_3 (II) phase.
- [22] R. A. Forman, B. A. Weinstein, and G. Piermarini, in *Spectroscopie des Éléments de Transition et des Éléments Lourds dans les Solids*, Lyon, France, 1976 (Centre National de la Recherche Scientifique, Paris, 1977).
- [23] T. Goto, T. J. Ahrens, and G. R. Rossman, *Phys. Chem. Mineral.* **4**, 253 (1979).
- [24] D. P. Ma, Y. Y. Liu, D. C. Wang, and J. R. Chen, *J. Phys. Condens. Matter* **7**, 4883 (1995).
- [25] L.-G. Liu and W. A. Bassett, *Elements, Oxides, and Silicates: High Pressure Phases with Implications for the Earth's Interior* (Oxford Press, New York, 1986), p. 126.
- [26] P. W. Bridgman, *Am. Acad. Arts Sci.* **72**, 45 (1937).
- [27] S. Minomura and H. G. Drickamer, *J. Appl. Phys.* **34**, 3043 (1963).
- [28] G. K. Lewis and H. G. Drickamer, *J. Chem. Phys.* **45**, 224 (1966).
- [29] W. Duan, R. M. Wentzcovitch, G. Paiva, and A. Fazzio (to be published).
- [30] H. d'Amour, D. Schiferl, W. Denner, H. Schulz, and W. B. Holzapfel, *J. Appl. Phys.* **49**, 4411 (1978).
- [31] R. W. G. Wyckoff, *Crystal Structures* (Interscience, New York, 1964), Vol. 2.
- [32] D. R. Stephens and H. G. Drickamer, *J. Chem. Phys.* **35**, 427 (1961).